DEVELOPMENT OF MUCOADHESIVE SILK FIBROIN NANOPARTICLES FOR SUSTAINED DRUG DELIVERY TO THE OCULAR SURFACE

CHULA SRIKAJORN

A Thesis Submitted to the Graduate School of Naresuan University
in Partial Fulfillment of the Requirements
for the Master of Science in (Biomedical Sciences - (Type A 2))
2020

DEVELOPMENT OF MUCOADHESIVE SILK FIBROIN NANOPARTICLES FOR SUSTAINED DRUG DELIVERY TO THE OCULAR SURFACE

CHULA SRIKAJORN

A Thesis Submitted to the Graduate School of Naresuan University
in Partial Fulfillment of the Requirements
for the Master of Science in (Biomedical Sciences - (Type A 2))
2020

Thesis entitled "Development of mucoadhesive silk fibroin nanoparticles for sustained drug delivery to the ocular surface"

By CHULA SRIKAJORN

has been approved by the Graduate School as partial fulfillment of the requirements for the Master of Science in Biomedical Sciences - (Type A 2) of Naresuan University

Oral Defense Committee

..... Chair
(Wudtichai Wisuitiprot, Ph.D.)

..... Advisor
(Wanachat Thongsuk, Ph.D.)

..... Co Advisor
(Associate Professor Waree Tiyaboonchai, Ph.D.)

..... Internal Examiner
(Assistant Professor Pussadee Paensuwan, Ph.D.)

..... External Examiner
(Wudtichai Wisuitiprot, Ph.D.)

Approved

.....
(Professor Paisarn Muneesawang, Ph.D.)

Dean of the Graduate School

Title	DEVELOPMENT OF MUCOADHESIVE SILK FIBROIN NANOPARTICLES FOR SUSTAINED DRUG DELIVERY TO THE OCULAR SURFACE
Author	CHULA SRIKAJORN
Advisor	Wanachat Thongsuk, Ph.D.
Co-Advisor	Associate Professor Waree Tiyaboonchai, Ph.D.
Academic Paper	Thesis M.S. in Biomedical Sciences - (Type A 2), Naresuan University, 2020
Keywords	nanoparticles, ocular drug delivery, mucoadhesive, chitosan, silk fibroin

ABSTRACT

Presently, the conventional eye drops are the most popular dosage forms for ocular drug delivery, especially for the treatment of anterior segment disorders. Because of it is convenient and non-invasive. However, after topical administration, the rapid clearances of the drug by blink-induced tear drainage and tear dilution are common cause of poor drug absorption and low bioavailability. Therefore, to overcome these limitations, in this study, silk fibroin nanoparticles (SFNs) were developed as a mucoadhesive nanocarrier for topical drug delivery to the ocular surface, that are able to enhance drug retention on the ocular surface and reduce drug elimination. SFNs were easily prepared by nanoprecipitation technique by dropping silk fibroin (SF), a negatively charged polymer, in 95% (v/v) ethanol. After that, the nanoparticle was separated and their surface was coated with chitosan (CS), a positively charged polymer, by polyelectrolyte complexation technique. Finally, polyethylene glycol 400 (PEG400), a stabilizing agent, was also added as a stabilizing agent. The effects of the volume ratios of SF:Ethanol and the amounts of CS and PEG400 on the physiological property, including morphology, particle size and surface charge of SFNs were evaluated. The entrapment efficiency (EE) was determined using sodium fluorescein (NaF) and nile red (NR) as examples of hydrophilic and hydrophobic drugs, respectively. Fourier transform infrared spectroscopy spectra (FTIR) confirmed the intermolecular interactions between the

positively charged amine groups of CS with the negatively charged sulfate group of SF. Mucoadhesiveness of nanoparticles was assessed *ex vivo* using porcine eyes. Whereas cell cytotoxicity study and cellular uptake were also determined *in vitr*o using human corneal epithelium cells line (HCEC)

The optimized condition for SFNs synthesis was a volume ratio of SF:Ethanol as 1:2 and the amounts of CS (C) and PEG400 (P) as 0.625 and 0.032 mg/ml, respectively, as called SFN-CP4. The SFN-CP4 were nearly spherical with size 198.47 ± 35.54 nm and surface charge as 38.33 ± 0.67 mV. Results of a comparison between the FTIR spectra of CS and SFN-CP4 were clearly indicated that the SFN-CP4 were coated with CS by peaks shifts of amide group in CS-FTIR spectra. The highest EE of NaF and NR into SFN-CP4 was ~95% and ~67%, respectively. SFN-CP4 showed long-term adherence to the surface of porcine cornea over 240 min. It entry into the HCEC within 30 min without induced cytotoxicity. Overall, the characteristics of SFN-CP 4 make them suitable for application in topical ocular surface drug delivery. Moreover, it can be adopted for delivery other drugs to improve therapeutics effect for ocular surface diseases.

ACKNOWLEDGEMENTS

I wish to express my deepest sincere appreciation to my advisor, Dr. Wanachat Thongsuk, for her constructive guidance, patience, inspiring word, understanding and her insights in ocular pharmaceutical sciences. I am thankful to my co-advisor, Associate Professor Dr. Waree Tiyaboonchai, for her encouragement and invaluable advisor. I am indeed deeply grateful to all the two advisors for having always believed in my abilities and for their concern in my progress and problems. They provided several opportunities along this journey. Their friendship and affection are heartfelt and an always thankful to them.

Also, I would like to acknowledge to Associate Professor SP Srinivas from Indiana University (Bloomington, USA), for his useful guidance, intellectual support, and suggestions for my thesis.

I am also thankful to Assistant professor Dr. Pussadee Paensuwan and Dr. Wudtichai Wisuitiprot for being members of my internal and external examination committees, respectively.

I am also thankful to all staff in the Faculty of Allied Health Sciences, Pharmaceutical Sciences and Sciences, Naresuan University, for their help throughout my study here at Naresuan University.

Lastly, but definitely not the least, I extend my sincere thanks to my parents for all their sacrifice in providing me the best possible education. Words are not enough to express my devotion and gratitude towards them, and I hope I get same blessings, love, and care from them for the rest of my life. Also, I have a great respect and gratitude college, who have been a constant motivation and have been there with me during my tough time.

CHULA SRIKAJORN

TABLE OF CONTENTS

Page

LIST OF TABLES

Page

LIST OF FIGURES

Page

CHAPTER I

INTRODUCTION

This chapter contains three parts including the rational for the study, the objective and the expected outputs of the study. The details of each past are the following:

The rational for the study

The eyes are an important organ for eyesight, if the eyes are damaged, especially the damaged of the ocular surface, it causes vision loss or blindness. Presently, the treatment of ocular surface via topical administration as an eye drops solution are the most common treatment options and usually prescribed by an eye specialist. However, after apply to the ocular surface, the drug may run off very quietly, due to rapid clearance (half-life <4 min) by the blink-induced tear drainage into the nasolacrimal system (1-3), lead to low ocular bioavailability. Thus, the patients need to apply eye drop more often, which may increase the risk of systemic side effects due to increase dosage (2). Therefore, to overcome the limitations of the conventional eye drops and increase the ocular bioavailability, an ideal eye drop formulation should be adhere and prolonged the residence time at ocular surface, reduced drug elimination, and controlling drug release (4).

Currently, the nano drug delivery system is engineered technology that used nanoparticle in the size ranges from 1 to 1,000 nm as dung carrier (5, 6). The drug molecules can be either entrapped within the particle or bound to their surface. Alternatively, several studies have shown promising results with mucoadhesive nanoparticles to enhance the resident time at the target site, which particularly useful because their surface properties can be modified (7). Thus, this is the one possibility of the mucoadhesive nanoparticle to increase the ocular bioavailability by enhance the resident time at the ocular surface. The usage of mucoadhesive polymers in the form of nanoparticles is a potential strategy. The mucoadhesive nanoparticles can reduce the drug drainage rate and prolong the residence time by adhere their positively charged surfaces with the negatively charged mucus at ocular surface

through electrostatic interaction (1, 2, 4). Silk fibroin (SF) (pKa~5), a negative charge polymer, is an interesting neural biopolymer that is being used in ophthalmic formulations due to its present excellent properties, such as biocompatibility, biodegradability, and low immunogenicity (8, 9). Moreover, it has been used as a mucoadhesive polymer even it presented a negatively charged properties (10). On the other hand, chitosan (CS) (pKa~6.5) is a natural hydrophilic positively charged polysaccharide that advantage of being non-toxic, biocompatible, and biodegradable. CS is excellent mucoadhesive properties that ability establishes electrostatic attraction, hydrogen, and hydrophobic bonding to mucin (11, 12). These features make CS an excellent candidate for various pharmaceutical and biomedical fields (13).

Therefore, the objective of this study is to develop mucoadhesive silk fibroin nanoparticles coating CS and PEG400 (SFN-CP) for sustained drug delivery to the ocular surface. In this study, SFN-CP were developed by using precipitation and polyelectrolyte complexation techniques (2). SF was formed as silk fibroin nanoparticles (SFNs) by precipitate in ethanol, while CS was coated on the surface of SFNs to provide the positive surface charge via polyelectrolyte complexation technique. Polyethylene glycol 400 (PEG 400) was used as a stabilizer agent for prevent self-aggregation. The effects of the volume ratios of SF:Ethanol and the amounts of CS and PEG400 on the physiological property, including morphology, particle size and surface charge of SFN-CP were evaluated. The entrapment efficiency (EE) was determined using sodium fluorescein (NaF) and Nile red (NR) as examples of hydrophilic and hydrophobic drugs, respectively. Fourier transform infrared spectroscopy spectra (FTIR) confirmed the intermolecular interactions between the positively charged amine groups of CS with the negatively charged sulfate group of SF. Mucoadhesiveness of SFN-CP was assessed ex vivo using porcine eyes. Whereas cell cytotoxicity study and cellular uptake were also determined in vitro using Human corneal epithelium cells line (HCEC). Overall, the SFN-CP were developed for topical drug delivery to the corneal surface by stepping over the limitations of the drug removal of the eye.

The objective of the study

To develop mucoadhesive silk fibroin-chitosan nanoparticles for sustained drug delivery to the ocular surface.

The expected output of the study

The expected output of this study is to obtain the mucoadhesive SFN-CP for topical ocular delivery. This SFN-CP model can be reduced the drug drainage rate and enhanced the drug retention time at the ocular surface. It can be useful in treatment of anterior segment eye disease and can be adopted for other therapeutic agents to improve residence time and thereby, intraocular bioavailability for diseases such as glaucoma and dry eye disease.

CHAPTER II

THEORETICAL AND RELATED LITERATURE

1. Anatomy of the eye

The eye is a complex organ consisting of sensitive tissue structures arranged as compactly adjoined layers (14). The eye is divided into two segments; (Figure 1) the anterior segment, which consist of tear film, cornea, conjunctiva, iris, ciliary body, lens and anterior sclera and the posterior segment consist of posterior sclera, choroid, Bruch's membrane, retina and vitreous humor. It composes of many complex layers and structures with a variety of defense mechanisms. These defense mechanisms as barriers design to protect the eye against foreign particles, molecules, and infectious organisms, include inhibit the movement of drugs into the eye (6).

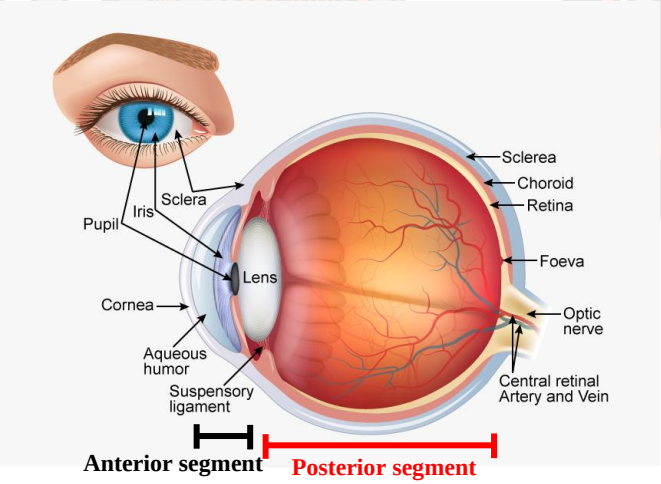

Figures 1 Anatomy of the human eye

Source: https://www.kindpng.com/imgv/ihhxwiR_structure-of-human-eye-class-10-hd-png/

1.1 Cornea

The cornea is located at the front of the eye. It is a transparent connective tissue that, along with the lens, allows the light to break into the eye (15). The cornea is composed of proteins and cells. It is avascular tissue due to blood vessels prevent it from refracting light properly and may adversely affect vision. Therefore, the cornea obtain nutrients and oxygen are supply from tear and aqueous humor. It is about horizontal diameter of the cornea typically measures about 12 mm, and the vertical diameter is 11 mm. The center thickness of the average cornea is about 0.5 mm and compose of five layers (Figure 2) (Corneal epithelium, Bowman’s layer, Stroma, Descemet's membrane, corneal endothelium)

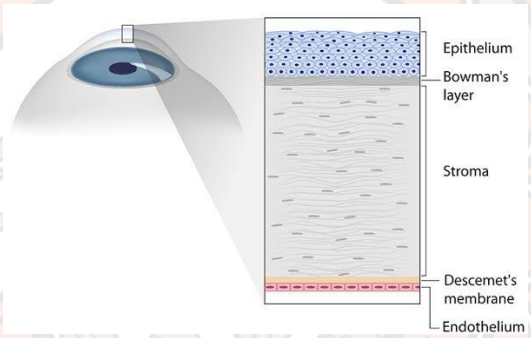

Figures 2 Cornea structure

Source: https://www.wilmingtoneye.com/specialties/cornea/structure-of-the-cornea

1.1.1 The corneal epithelium

Corneal epithelium is an outer layer of the cornea, measures about 50 µm thick and making it slightly less than 10 percent of the thickness of the entire cornea. corneal epithelial cells are constantly being produced and sloughed off in the tear layer of the surface of the eye. It provides an optimal surface for the tear film to spread across the surface of the eye to keep it moist and healthy and to maintain clear, stable vision.

1.1.2 Bowman's layer

Bowman's layer is a very thin (8 to 14 µm) and dense fibrous sheet of connective tissue that forms the transition between the corneal epithelium and

the underlying stroma. It prevents corneal scratches from penetrating the corneal stroma. Corneal abrasions that are limited to the outer epithelial layer generally heal without scarring, but scratches that penetrate Bowman's layer and the corneal stroma typically leave permanent scars that can affect vision.

1.1.3 Corneal stroma

Corneal stroma is the middle layer of the cornea is approximately 500 μm thick, or about 90 percent of the thickness of the overall cornea. It is composed of collagen fibrils. These fibrils are uniform in size and arranged parallel to the corneal surface in 200 to 300 flat bundles called lamellae. The regular arrangement and uniform spacing of these lamellae are what enable the cornea to be clear.

1.1.4 Descemet's membrane

Descemet's membrane is a very thin layer separates the stroma from the underlying endothelial layer of the cornea.

1.1.5 Corneal endothelium

Corneal endothelium is the innermost layer of the cornea. It is only a single layer of cells thick and measures about 5 microns. Most of the endothelial cells are hexagonal. The endothelium maintains the fluid content within the cornea. Damage to the corneal endothelium can cause swelling that can affect vision and corneal health.

1.2 Conjunctiva

The conjunctiva is a thin membrane and clear that covers part of the front surface of the eye and the inner surface of the eyelids. It has two segments such as bulbar conjunctival and palpebral conjunctival. The conjunctival maintain moist and lubricated eye surface and protect the eye from dust, debris and infection-causing microorganisms. The conjunctiva has many small blood vessels that provide nutrients to the front eye surface. It also secretes a component of the tear film to help prevent dry eye syndrome.

1.3 Iris

The iris is the thin, circular structure that consists of connective tissue and muscle that surrounds the pupil. The color of our eyes is determined by the amount of pigment in the iris. Moreover, it still acts like the diaphragm of a camera and controls the size of the pupil. When bright lighten, muscle of iris constricts the pupil and in contrast, when dim lighting or the dark, muscle of iris dilates the pupil.

1.4 Ciliary body

The ciliary body surrounds the iris, holds the lens of the eye in place. It is connected to the lens with zonules of Zinn that suspend the lens in place behind the pupil to controls accommodation. The ciliary body also generate the aqueous humor.

1.5 Retina

The retina plays a vital role in fine detailed visual acuity and color vision. The primary function of the retina is to process visual information as well as control image formation (16). The retina is the sensory membrane composed of multilayers; it lines the inner surface of the back of the eyeball. The retina has specialized cells called photoreceptors. Photoreceptors cells take light focused by the cornea and lens then convert into chemical and nervous signals transported to visual centers in the brain via the optic nerve to converted signals into images and visual perceptions. The photoreceptor cells have two types consist Rod cells located throughout the retina, that act as detect motion, obtain black-and-white vision and function well in low light. Cone cell located in a small central area of the retina called the macula. At the center of the macula is a small depression, called the fovea. The fovea contains only cone photoreceptors and it is the point in the retina responsible for maximum visual acuity and color vision. It performs best in medium and bright light.

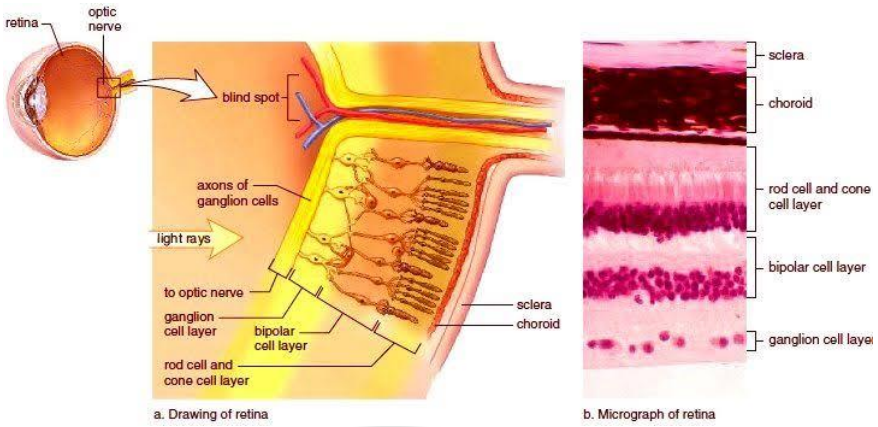

Figures 3 Retina structure

Source: http://encyclopedia.lubopitkobg.com/Anatomy_and_Physiology_of_the_Eye.html

2. Barrier properties for topical drug administration

The first barrier mechanism involves the anterior segment of the eye, such as the eyelid and lashes. These structures, along with the body's blinking reflex, can defend the eye against particles. This blinking reflex plays a role in rapidly removing the formulation of current ocular drug delivery systems from the surface of the eye and not allowing the drug enough time to penetrate through the barriers (6).

Topically drug administered, targeting the ocular inner tissues, discover static, dynamic and metabolic barriers that limit ocular bioavailability. These barriers can be classified as precorneal and corneal (17).

2.1 Precorneal barriers

Tear drainage forms a major precorneal barrier component, the conjunctival cul-de-sac of the eye can support eye drop, about 7 to10 µl fluid. thus, it is an important portion of the topically administered eye drop of 35–50 µl, is lost. In additional, tear drainage causes the removal of the eye drop from tear secretion, which is normal tear volume on the corneal surface about 7±2 ml and the rate of secretion of the tears has been as 1.2 ml/min (17-19). Therefore, the increased tear flow can lead to faster precorneal elimination and decreased efficacy. Also,

osmolarity and pH of the drug formulation are important parameters that can induce tear generation (17).

The tear film is pre-corneal film consists of three layers such as an outer lipid layer, a middle aqueous layer, and an inner mucous layer (Figure 4). This is the first and foremost ocular barrier that is encountered after topical administration of a therapeutic agent. Tear film has a high turnover rate and is continuously secreted by the lacrimal gland and drained into the nasolacrimal duct. Its main function is to moisten the superficial ocular tissues in order to prevent drying. The continuous secretion and drainage of tear fluid readily clear topically administered drugs from the ocular surface, resulting in low bioavailability in the underlying ocular tissues (1-3, 14). Hence, the tear film is considered as a dynamic ocular barrier. The hydrophilic and hydrophobic of drug molecules govern their interaction with tear fluid (20). Hence, the physicochemical properties of drug molecules and delivery systems and their interaction with tear fluid together govern the ability of the drug molecule to traverse through the tear film barrier and interact with the subsequent tissue, cornea (21).

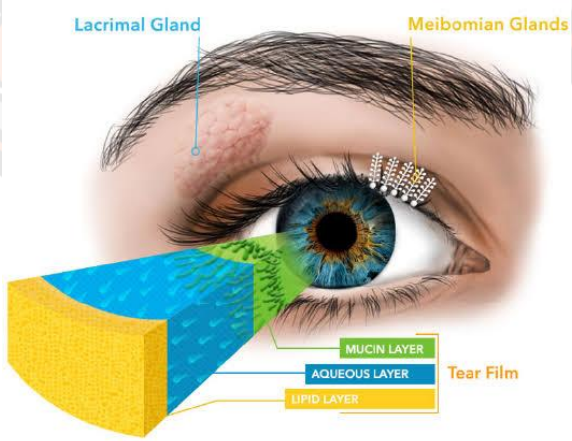

Figures 4 Tear film structure

Source: https://www.dryeyes.vision/thai/thai_dryeyes.html

2.2 Corneal barriers

The cornea forms one of the major barriers for the transport of substances into the eye. It is a multilayered barrier limiting drug penetration into the aqueous humor. The cornea is transparent front past of the eye that contains five layers such as epithelium, Bowman's membrane, stroma, Descemet's membrane, and endothelium. Which each layer has lipophilic and hydrophilic characteristics consist of the epithelium and endothelium are lipophilic in nature (Figure 5), whereas stroma is hydrophilic in nature (17). Therefore, the drug should have appropriate hydrophilicity/lipophilicity and other physicochemical property for penetration across the cornea. Also, the corneal epithelial cells have tight junctions (Figure 6) that limit across corneal paracellular diffusion, especially many types of hydrophilic molecules (13). The corneal stroma is mostly composed of charged and highly organized hydrophilic collagen fiber that closely ranged together. It is not only an effective barrier to most microorganisms but also for drug absorption (16). The corneal endothelium is an innermost layer, which is a monolayer of hexagonal endothelial cells to adjust balance water influx into the cornea and a barrier between the cornea and aqueous humor. It is presenting little restriction to the movement of macromolecules between the stroma and aqueous humor. Thus, the corneal epithelium acts as the major barrier to across corneal diffusion of drug.

The washing of eye drops which is applied to the eye is largely due to the rapid turnover rate of lacrimal fluid. This results in the eye drop eliminate from the surface of the eye to the nasolacrimal duct system within 4 minutes.

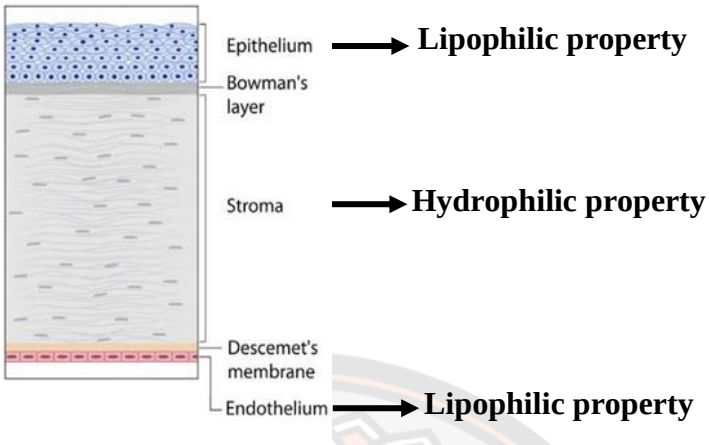

Figures 5 Corneal layer property

Source: https://www.researchgate.net/figure/3-Diagram-of-the-cross-section-of-the-cornea-showing-the-five-different-layers-The_fig3_305441043

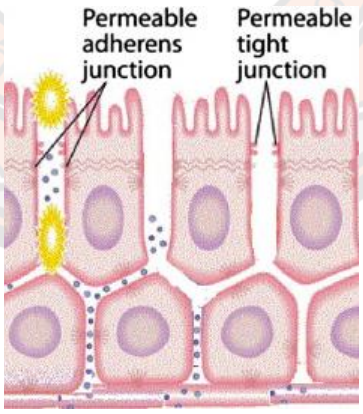

Figures 6 Cornea epithelium tight junction

Source: https://www.researchgate.net/figure/Structure-of-corneal-epithelial-tight-junctions-and-possible-way-of-SiNPs-to-penetrate_fig1_259173728

3. Ocular treatments for anterior segment

Treatment to the anterior segment of ocular diseases often use topical administration as route is the only noninvasive route, is the most preferred route of dosing for anterior segment ocular diseases (17). Whereas all other routes are invasive in nature. Furthermore, drug administration via subretinal, sub-choroidal and intravitreal injections involve a high risk as these routes of administration can lead to retinal detachment. Hence, the topical route is preferred as this noninvasive route improves patient compliance. The currently on the market, they can find that conventional topical ophthalmic formulations include eye drops (solutions, suspensions) and ointments.

3.1 Eye Drops

Eye drops, one of the most widely used pharmaceutical forms, are directly administered to the eye surface due to safety, take immediate action after applied, have high patient-compliance, are suitable for the product and above all, are non-invasive (18, 19). The current first treatment for many ocular diseases, particularly those affecting the anterior segment of the eye, is eye drops (6).

The eye drops as a solution form, are performance characteristics by a permeation of the supported drug by a pulsatile mechanism which occurs after the topical instillation of the drops, with further quick declination of the drug concentration following a kinetic profile corresponding roughly to a first-order elimination process (18). Topical administration of drops to the eye, it is important to consider the limit to dosage that the conjunctival cul-de-sac of the eye can support eye drop; about 7 to10 µL. It has been shown that approximately 10% of an administered dose of eye drops (~50 µL) (6, 17) will penetrate the eye and reach the target site at an effective concentration. This reason leads to frequent dosage form. In additional, the topical eye drop is rapidly removed from the ocular surface leading a short drug retention time. Normally, less than 5% of the drug administered is retained on the ocular surface as a result of the corneal epithelium barrier and nasolacrimal system (16).

Although, eye drops allow the patient to administer their medication themselves at home. However, there are limitations to this, due to very short retention

time at the eye surface, low bioavailability, less stability of the dissolved drug, requirement of preservatives, leading to toxicity, and rapid clearance of these formulations Therefore, to expand the time of contact of the drug, the capacity of permeation and high bioavailability of the drug, in which several modifiers are employed in optimizing eye drops, such as polymers and nanoparticles that can be enhancers of viscosity and of permeability.

3.2 Ointments

Topical formulations ointments are used too as carrier systems for drug delivery to anterior segment treatments. The melting points of ointment often near to the ocular temperature of 34°C (6, 17) to reach the target site. It has been developed extensively to date, due to it has advantages of the viscous nature of the formulation, they are not washed away from the eye as rapidly as liquid formulations compare with eye drop formulation and resulting in a higher bioavailability. However, this viscosity also leads to blurred vision and unstable dosage. Although ointments are advantageous in terms of bioavailability, not investigated as extensively as other ophthalmic formulations in the form of nanoparticle.

3.3 Suspensions

Ocular suspensions are a dispersion of finely divided insoluble drug particles suspended in an aqueous medium containing dispersing and solubilizing agents. The pre-corneal can be retained drug particles in suspension enhancing the contact time of the drug. The particle size of the drug determines the time required for the absorption of the drug molecules into corneal tissue thus ultimately affecting the drug bioavailability.

3.4 Emulsions

An emulsion is a biphasic system composed of two immiscible phases. Ophthalmic emulsions can offer advantages of improvement in drug solubility and bioavailability of previously water-insoluble drugs. Pharmaceutical emulsions can be widely categorized as water in oil (w/o) and oil in water (o/w). Ophthalmic formulations widely utilize the o/w system, which consists of a hydrophobic drug

mixed in oil and dispersed in an aqueous medium. An o/w emulsion is preferred over a w/o emulsion for the reasons of better ocular tolerability and lower ocular irritation due to the external aqueous phase.

4. Nanoparticles for ocular drug delivery

Nanoparticles have a wide variety of uses, across several fields. Regarding the medical field, they have been extensively investigated and developed to aim in both diagnosis and treatment of diseases. It provides novel opportunities to overcome the limitations of conventional drug delivery systems through the nanostructures that capable of encapsulating and delivering drug molecules. Nanoparticles are described as materials with a range of 1–1000 nm in at least one dimension (5, 6), also in nanomaterials definition are objects in the range of 1 and 100 nm and exhibit dimension-dependent phenomena such as the quantum-size effect (16). However, generalized definition, the nanoparticles with drug loading have small sizes ranging from 1 to 1000 nm and can control the release of therapeutic agents and enhance penetration through different biological barriers of the eye. Also, the nanoparticles have been shown to ensuring low eye irritation, mucoadhesive property, improving drug bioavailability or enhancing ocular tissue compatibility (22). One of the major benefits of nanoparticle in ocular drug delivery is their ability to adhere to mucosa on the ocular surface and epithelium surrounding the eye, also preventing formulations from being almost immediately eliminated by defense mechanisms (6). Drug-loaded nanoparticles with size ranging from 50 to 400 nm are considered versatile for ocular delivery as they have the ability to overcome physiological barriers and to direct the drug to specific cells, either by passive or ligand mediated targeting mechanisms.

5. Mucoadhesion drug delivery

Mucoadhesion as the interaction between a mucin surface and a synthetic or natural polymer (23-26). Mucoadhesion has shown prolonging the residence time of mucoadhesive dosage forms through various mucosal routes in drug delivery applications. Mucoadhesive based topical systems have shown increased bioavailability. Mucoadhesive drug delivery provided great absorption and bioavailability due to its considerable surface area and high blood flow. Therefore,

mucosal drug delivery system could be of value in delivering a growing number of high-molecular-weight sensitive molecules such as peptide and oligonucleotides.

5.1 Mucoadhesive material

Mucoadhesive polymers have various hydrophilic groups, such as hydroxyl, carboxyl, amide, and sulfate. This groups can be attached to mucus or the cell membrane by various interactions such as hydrogen bonding and hydrophobic or electrostatic interactions. These hydrophilic groups also cause polymers to swell in water and, thus, expose the maximum number of adhesive sites. The polymer for a bioadhesive, drug delivery system has to the following characteristics:

- Degradation products should be nontoxic and nonabsorbable.
- Nonirritant.
- Can form a strong non-covalent bond with the mucus or epithelial cell surface.
- Adhere to mucus tissue and possess some site-specificity.
- Allow easy incorporation of the drug and offer no hindrance to its release.
- Not decompose on storage or during the shelf life of the dosage form.
- The polymers can be adhered to biological surfaces can be divided into three categories:
- Adhere through nonspecific, noncovalent interactions which are primarily electrostatic in nature.
- Polymers possessing hydrophilic functional groups that hydrogen bond with similar groups on biological substrates.
- Polymers that bind to specific receptor sites on the cell or mucus surface

5.1.1 Silk fibroin (SF)

The silk fibroin is a natural fibrous protein, is a more biocompatible biomaterial than some commonly used biological polymers such as collagen and poly(l-lactic acid) (PLA) (27). The application of SF as a biomaterial began centuries ago, with its use as sutures for wound treatment. Due to their

excellent performance, SF-based biomaterials have been found suitable for a variety of applications, including drug delivery (1, 2, 21), vascular tissue regeneration, skin wound dressing, and bone tissue scaffolds (28, 29). Silk fibroin was recognized by the US Food and Drug Administration (FDA) as a biomaterial in 1993 (28). Compared with other natural biopolymers, SF is promising due to its excellent mechanical properties, good biocompatibility, biodegradability, and the versatility of structural re-adjustments. These advantageous properties are attributed to its unique physicochemical properties (27).

SF is used as a polymer in nanoparticle for ocular drug delivery system, it has been shown to increase the retention time of the drug administered due to mucoadhesive properties, less cytotoxicity and good antifungal (30). In addition, the silk fibroin can interact ionically with an oppositely charged molecule can take advantage of topical drug delivery on the ocular surface (31). For example, this formulation used the electrostatic interactions technique between silk fibroin and liposomes to develop topical delivery. The result showed the silk fibroin promote a potential mucoadhesive biopolymer to enhance residence time of drug on the eye surface (9).

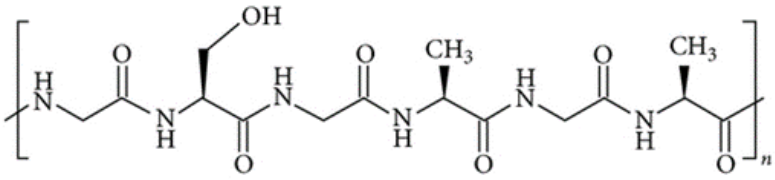

Figures 7 Silk Fibroin chemical structure

Source: https://www.researchgate.net/figure/Chemical-structures-of-a-silk-fibroin-b-alginate-and-c-tetracycline-hydrochloride_fig1_258393198

5.1.2 Chitosan (CS)

Chitosan is abundant polysaccharide in nature, it is obtained from the deacetylation of chitin. Chitin is a cationic amino polysaccharide made up of N-acetyl D-glucosamine (GlcNAc) repeat blocks, joined by β-1, 4 glycosidic bonds

(32). Chitin is extracted from the exoskeletons of crustaceans and predominantly from shrimp crabs and cell walls of fungi and yeasts, and the spines of diatoms. It is highly hydrophobic then insoluble in water (soluble in acidic mediums) and most organic solvents. Moreover, chitosan has several great characteristics, it is a bioactive polymer with antibacterial activity including non-toxicity, easy modification, mucoadhesive and biodegradation (4, 6, 33). In addition, makes widely used in medicine, food, water treatment, and other fields (34). These features make CS an excellent candidate for various pharmaceutical and biomedical fields (13).

CS is often used as a polymer in ophthalmic preparations due to It is a cationic polysaccharide, then it to react with the negative charges found within the mucus of ocular surface and conjunctiva. It has been shown to increase the retention time of the drug administered and improve the penetration of the corneal surface due to its mucoadhesive property and ability to open tight junctions (6, 16). CS is being developed into a variety of nanoparticle formulations to treat ocular disease, such as nanoparticle to treat glaucoma, conjunctivitis as well as multiple immune-related ocular degeneration (4, 6).

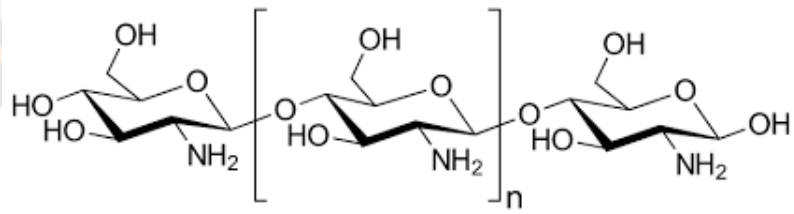

Figures 8 Chitosan chemical structure

Source: https://commons.wikimedia.org/wiki/File:Chitosan_chemical_structural _formula.svg

5.2 Ocular mucoadhesive drug delivery systems

Mucoadhesion is commonly defined as the adhesion between two materials, at least one of which is a mucosal surface. Mucoadhesive dosage forms

may be designed to enable prolonged retention at the site of application, providing a controlled rate of drug release for improved therapeutic outcome. Application of dosage forms to mucosal surfaces may be of benefit to drug molecules not amenable to the oral route, such as those that undergo acid degradation or extensive first-pass metabolism. The mucoadhesive ability of a dosage form is dependent upon a variety of factors, including the nature of the mucosal tissue and the physicochemical properties of the polymeric formulation. This review article aims to provide an overview of the various aspects of mucoadhesion, mucoadhesive materials, factors affecting mucoadhesion, evaluating methods, and finally various mucoadhesive drug delivery systems (23).

Drug administration to the eye is a challenge because there are several mechanisms such as tear production, tear flow, and blinking. These induced protect the eye from the harmful agents including eye drops. Conventional delivery methods have low efficiency. Solutions and suspensions are readily washed from the eyes and ointments alter the tear refractive index and blur vision. Therefore, it is a target to prolong the residence time by mucoadhesion.

CHAPTER III

RESEARCH METHODOLOGY

Materials

1. Calcium chloride ($CaCl_2$) (Cat No. AR1235, Labscan, Bangkok, Thailand)
2. Calcium nitrate ($Ca(NO_3)_2$) (Cat No. 202967, Sigma-Aldrich, USA)
3. Ethanol (Cat No. AR1069-P4L, Labscan, Bangkok, Thailand)
4. Degummed silk yarns of *Bombyx mori* (Collected from Bondin Thai Silk Khorat Co., Ltd, Thailand)
5. Chitosan shrimp (CS) (Obtained from Aquapremier, Inc., Bangkok, Thailand)
6. Glycerol (obtained from the sun chemical Co., Ltd, Bangkok, Thailand)
7. Polyethylene Glycol (PEG 400) (Obtained from Nam Siang Co., Ltd, Bangkok, Thailand)
8. Nile red (NR) (Cat No. N1142, Invitrogen, USA)
9. Sodium fluorescein (NaF) (Cat No. F6377, Sigma-Aldrich, USA)
10. Keratinocyte Serum-Free Growth Medium (K-SFM) (Cat No. 17005042, Gibco, USA)
11. Resazurin (Cat No. 424701, BioLegend, USA)
12. Phosphate Buffered Saline (PBS) (Cat No. P4417, Sigma-Aldrich, USA)
13. Dimethyl sulfoxide (DMSO) (Cat No. 276855, Sigma-Aldrich, USA.)
14. Fluorescein isothiocyanate (FITC) (Cat No. F7250, Sigma-Aldrich, USA)
15. Ethylenediaminetetraacetic acid (EDTA) (Cat NoE9884, Sigma-Aldrich, USA)
16. 4′,6-diamidino-2-phenylindole (DAPI) (Cat No. D9542, Sigma-Aldrich, USA)
17. Methanol (Cat No. AR1115-P5L, Labscan, Bangkok, Thailand)
18. 4% paraformaldehyde (Cat No. 158127, Sigma-Aldrich, USA)
19. Tween 80 (Cat No. TB0562, Bio basic, Canada)

Apparatus

1. Freeze dryer (Heto PowerDry LL3000, Thermo Fisher, USA)
2. Homogenizer (Ultra Turrax T25, IKA, Germany)
3. Incubator (Shel lab Model 2424, USA)

4. Microplate reader (Bio-Rad, Hercules, CA, USA)
5. Scanning electron microscope (1455VP Leo, United Kingdom)
6. Dynamic light scattering (DLS) (Brookhaven Instrument, Holtsville, NY)
7. Centrifuge (MIKRO 220R, Hettich, Canada)
8. Shaker (3D sunflower mini, Latvla)
9. Fluorescence microscope (BX51, OLYMPUS, Japan)
10. Cryostat microtome (CM1850, Leica, USA)

Scope of study

The diagram illustrates of the research process is shown in Figure 9. Fibroin was extracted from yellow silk cocoon and used for preparing the silk fibroin-chitosan nanoparticles. Physicochemical characterization of the SFN-CP, such as morphology, particle size, surface charge, chemical reaction, and drug entrapment efficiency, was determined. After that, the optimized SFN-CP were evaluated for their possibility to adhere at the ocular surface by mucoadhesion study (*ex vivo*), tested their cytotoxic effect to corneal epithelial cells (*in vitro*) and also determined for their possibility to enter the cells (*in vitro*).

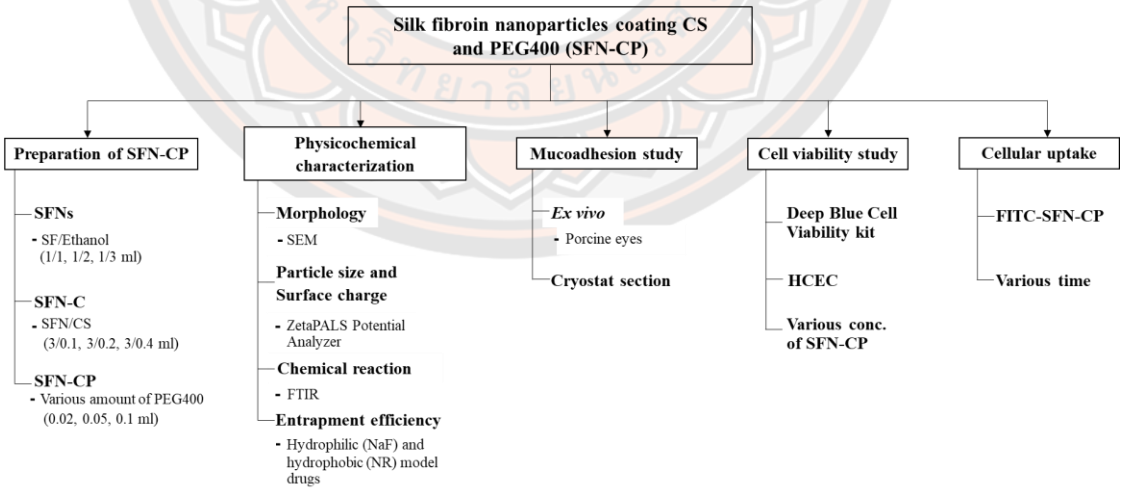

Figures 9 The diagram illustrates the process of preparation silk fibroin nanoparticles coating CS and PEG400 (SFN-CP) and investigates the properties of nanoparticles for drug delivery to the ocular surface.

1. Silk fibroin extraction

Silk fibroin (SF) solution was prepared by modified methods in previous literature (13, 14). Briefly, 5 g of degummed silk yarns was cut into short fibers and added in a mixed solution of $CaCl_2$: H_2O: $Ca(NO_3)_2$: EtOH at 30:45:5:20 weight ratio. After that, the wetted fibers were heated at 900 W in microwave for 2 min to form a clear solution. The result SF solution was dialyzed in a snakeskin pleated dialysis tube (10,000 MWCO, 22mm ID) against distilled water at room temperature for 3–5 days to remove salts. The aqueous SF solution was centrifuged at 10,000 rpm, 4°C for 30 min to remove the impurities, and silk aggregates formed during dialysis to clarify the solution. Following centrifugation, SF solution was lyophilized using a freeze dryer (Heto PowerDry LL3000, Thermo Fisher, USA) at 1×10^{-4} Torr and -55°C and kept in sealed plastic bags at -80°C.

2. Preparation of silk fibroin nanoparticles coating CS and PEG400 (SFN-CP)

SF solution (1%, w/v in DI water) was added dropwise into the ethanol with mild stirring (~500 RPM). The nanoparticles were obtained after stirring for 20 min and stored overnight at 4°C, resulting slightly viscous nanoparticles suspension. After centrifugation at 18,000 rpm for 30 min, the supernatant was removed and the compacted SFNs residues were washed with deionized water (DI water) two times by centrifugation method at 18,000 rpm for 30 min with a 20 µl glycerol bed at the bottom. The nanoparticles were re-dispersed in DI water, vortexed and subsequently sonicated twice for 30 sec at 40% amplitude. The effect of SF:ethanol ratios (Table 1) on the physiological properties of SFNs was investigated.

For preparing the SFN-C (Table 2), the obtained SFNs were coated with chitosan by adding chitosan solution (CS) (1%, w/v in DI water) to the SFNs dispersion under mild stirring at ~500 RPM at room temperature for 20 min. Finally, PEG400 was added slowly to the solution with continuous stirring ~500 RPM for 20 min, to prepare as the SFN-CP formulation. The final SFN-CP were washed two times with DI water by the centrifugation method.

In order to load the fluorescence into the nanoparticles, nile red (NR) and sodium fluorescein (NaF) were used as drug model, then an appropriate amount of

fluorescence was dissolved in 2.5 ml of silk fibroin (SF) solution and maintained for 2 hours before adding to ethanol.

All samples were prepared in triplicate. The unloaded-SFN-C were prepared as controls. The effect of ethanol:SF ratios on the physiological properties of SFN was investigated. Moreover, the influence of SFN/CS ratios and the amounts of PEG400 (Table 3) on the physicochemical properties of SFN-CP were also evaluated.

Tables 1 The volume ratios among SF and Ethanol for preparation of silk fibroin nanoparticles (SFNs)

Formulation	1% (w/v) Silk Fibroin (ml)	Ethanol (ml)	Total (ml)
SFN 1	1	1	2
SFN 2	1	2	3
SFN 3	1	3	4

Tables 2 The among of SFNs and CS for coating the nanoparticles (SFN-C) (when the ratio of SF:Ethanol was fixed as 1:2)

Formulation	1% (w/v) Silk Fibroin (ml)	Ethanol (ml)	1% (w/v) Chitosan (ml)	Total (ml)
SFN-C 1	1	2	0.1	3.1
SFN-C 2	1	2	0.2	3.2
SFN-C 3	1	2	0.4	3.4

Tables 3 The among of PEG400 for coating SFN-C (when the ratio SF:Ethanol was fixed as 1:2 and CS was fixed as 0.2 ml)

Formulation	1% (w/v) Silk Fibroin (ml)	Ethanol (ml)	1% (w/v) Chitosan (ml)	PEG400 (ml)	Total (ml)
SFN-CP 1	1	2	0.2	0.02	3.22
SFN-CP 2	1	2	0.2	0.05	3.25
SFN-CP 3	1	2	0.2	0.1	3.30

3. Physical characterization of SFN-CP

3.1 Morphology

The morphology of the nanoparticles were characterized by scanning electron microscopy (SEM) (1455VP; LEO Electron Microscopy Ltd., Cambridge, United Kingdom). The nanoparticles were dropped on studs with carbon tape, sputter-coated with gold, and then observed at a magnification of 10,000x.

3.2 Particle size and surface charge

The mean particle size and size distribution was measured by dynamic light scattering (DLS) using ZetaPAL/90plus (Brookhaven Instrument, Holtsville, NY). This instrument is equipped with a 35mW HeNe laser diode operating at 632.8 nm (JDS Uniphase, San Jose, CA) and a BI-200SM Goniometer with an EMI-9863 photomultiplier tube connected to a BI-9000AT digital correlator. An aliquot of SFNs were diluted in DI water. The particle size of each sample was measured at 25°C at a detection angle of 90° for 10 repeated measurements. Raw data was analyzed to obtain an average mean size by cumulative analysis.

The surface charge was determined by zeta potential using phase analysis light scattering with ZetaPAL/90plus (Brookhaven Instrument). Measurements were carried out at 25°C at 14.8° to the incident light. Samples was prepared by re-dispersing the SFNs in DI water. The zeta potential was calculated using the electrophoretic mobility based on the Smoluchowski approximation.

3.3 Chemical reaction

Fourier Transform Infrared Spectroscopy (FT-IR) analysis was performed in order to detect the possible structural changes of SFN-CP. The CS, SF, SFN 2 and SFN-CP 4 were evaluated. Each spectrum was acquired on a Tensor 27 spectrophotometer (Bruker Optics, Germany), equipped with a deuterated triglycine sulfate (DTGS) detector, by an attenuated total reflection (ATR) method, using a zinc selenide (ZnSe) crystal cell. Spectra were obtained under a dry air purge at coaddition of 256 interferograms collected at 4.0 cm^{-1} resolution and a wavenumber range of 4000–400 cm^{-1}. Empty cell was used to measure background signals and subtracted from the sample reading.

3.4 Entrapment efficiency

The entrapment efficiency (EE) of SFN-CP 4 was determined by separating free fluorescence (NR or NaF) from fluorescence loaded SFNs using cooling centrifuge method. The nanoparticles were centrifuge at 18,000 rpm, 4°C, for 30 min. After discarding the supernatant, the loading fluorescence was extracted from SFNs using ethanol and sonication for 1 min at room temperature. Then, the sample was centrifuge against at 18,000 rpm for 30 min at 4°C. The supernatant was analyzed by UV-Vis spectrophotometer at 575 nm for NR and 490 nm for NaF. Ethanol was used as blanks. The EE of NaF and NR into the nanoparticles were calculated as [(Amount of NaF/NR extracted) ×100]/(Initial amount of NaF/NR). The EE is reported as the mean of 3 independent trials.

4. *Ex vivo* mucoadhesion study

The retention of SFN-CP on the corneal surface was determined by using porcine corneal experiment. The nanoparticles were labelled with fluorescein isothiocyanate (FITC) based on the reaction of a primary amino group of CS with the isothiocyanate group of FITC as reported earlier. Briefly, the FITC solution (5 ml; 0.2% w/v: dissolved in methanol) was mixed with the CS solution (10 ml; 1% w/v: dissolved in 1.75% acetic acid) under mild stirring. Post mixing, 10 ml of methanol was added and stirred overnight in the dark, at room temperature. FITC-CS was precipitated by adding 25 ml of 0.2 M NaOH, centrifuged (at 5,000 RPM for 20 min),

and washed with methanol 3 times. The resulting FITC-CS was dissolved in 1.75% acetic acid solution to produce 1% w/v FITC-CS solution before adding to the SFNs as mentioned above. The FITC-labelled SFN-CP (FITC-SFN-CP) were washed 3 times in DI water.

Porcine eyes were obtained from a local slaughterhouse and corneas were isolated within 8 hours of death. Corneal buttons were cut out with a trephine from porcine eyes and it was held on glass slide support as Figure 10. FITC-SFN-CP were dropped in the central corneal and exposed to a continuous stream of NSS at rate 10 ml/min for 5 and 60 min. After that, the corneal cryostat sections were prepared and imaged with a fluorescence microscope (BX51, OLYMPUS, Japan).

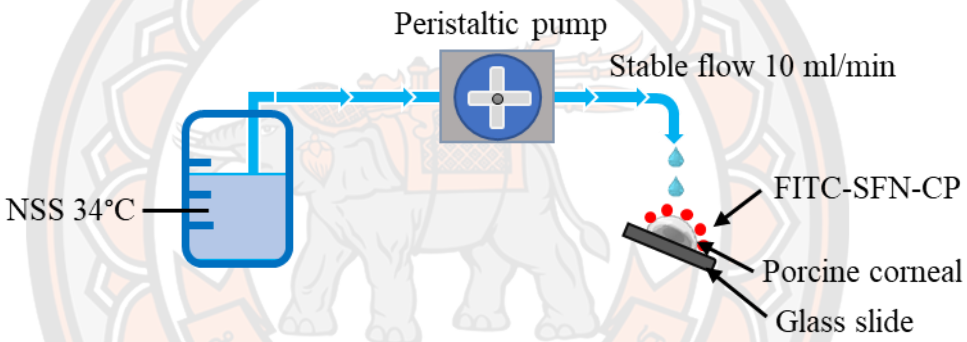

Figures 10 *Ex vivo* mucoadhesion studies

5. Human Corneal Epithelial cells (HCEC) culture

The HCEC cells were cultured in Keratinocyte Serum-Free Growth Medium (K-SFM) supplemented with 0.05 mg/ml bovine pituitary extract, 5 ng/ml human recombinant epidermal growth factor, 500 ng/ml hydrocortisone and 0.005 mg/ml bovine insulin into T25 cell culture flask at 37°C with 5% CO_2. The K-SFM was renewed every 2 days. The cells were observed daily by phase contrast microscopy (AxioImager Z1; Zeiss, Oberkochen, Germany).

6. Cell viability study

The HCEC cells, 2×10^4 cells/well, were seeded into 96-well culture plate, cultured until reaching the semi-confluence. Then, the cells were treated with different concentrations of SFN-CP for 24 hours. Cell viability was assessed by

the alamarblue cell viability assay. Briefly, the medium containing sample was removed and washed with PBS to removed sample that perched on the cell. After that, 100 µl of alarmablue reagent (medium and 10% alarmablue) was added to each well, followed by incubation for 3 h at 37°C in the dark. After incubation, remove the plate and measure the absorbance was measured spectrophotometrically at 590 nm using a microplate reader (Bio-Rad, Hercules, CA, USA). Positive control (100% no toxic) consisted of wells containing cell and K-SFM. Wells without cells containing K-SFM was served as negative control (0%, toxic). Cell viability (%) was calculated according to the following equation: Cell viability (%) = [absorbance of sample/absorbance of positive control] ×100. All data were expressed as the mean of three measurements.

7. Cellular uptake by HCEC cells

Twenty-two microliters of FITC-SFN-CP (0.063% w/v) were mixed with 478 µl of K-SFM and exposed to HCEC cells for 5, 30, 60 ,120 and 240 min, respectively. The cells were washed three times with ice-cold PBS to remove excess nanoparticles and then once with 5 mM EDTA (pH 5.0) for 15 min to remove membrane-bound nanoparticles. Cells were fixed for 15 min in 4% paraformaldehyde, rinsed in PBS, permeabilized using 0.5% Triton-X 100 in DI water for 15 min and stained with DAPI to visualize the nucleus. The stained cells were mounted on a glass slide using a mounting medium (Prolong Antifade; Molecular Probes), according to the manufacturer's instructions and observed using a fluorescent microscope. The untreated cells were exposed to K-SFM culture medium as a control.

8. Data Analysis

All quantification studies were performed in triplicate. The data are expressed as mean ± standard deviation and analyzed using the Student's t-test for determining the significance of the difference between the means of two sets of data. Differences are considered significant at the *p*-value is less than 0.05.

CHAPTER IV

RESULTS

1. Physical characterization of SFN-CP

In this study, the mucoadhesive silk fibroin-chitosan nanoparticles was successfully developed. The SEM images of SFNs were showed in Figure 11. The morphology of all SFNs formulations showed spherical particles with a smooth surface. Firstly, SFNs were generated with precipitation technique in Ethanol. The effect of SF:Ethanol volume ratios on the physical characterization of SFNs were investigated. DLS of SFNs showed a mean particle sizes ranging from 130 nm to 190 nm, depending on the ratios of SF:Ethanol, with PI <0.2. However, a trend of decreasing particle diameter size with increasing volume of Ethanol could be seen (Table 4). Moreover, as shown in Figure 12, SFN 2 and SFN 3 showed significantly smaller particle sizes than SFN 1 ($p<0.05$). In order to evaluate the surface charge of nanoparticles using phase analysis light scattering, all formulations showed similar negatively charged surfaces between -20.21 and -20.94 mV as shown in Table 4. However, the smallest size with vast number of nanoparticles could be only observed in SFN 2 formulation. Thus, SFN 2 was used for coating of CS and PEG400.

In order to form as SFN-C, the SFN 2 was coated with CS by polyelectrolyte complexation technique. As shown in Table 5, the DLS analysis showed a mean particle sizes ranging of SFN-C from 177 nm to 210 nm with PI <0.2, depending on the amount of CS. Surface charge of SFN-C showed positive zeta potential between +23.12 and +38.39 mV. SFN-C 3 showed the mean size smaller than 200 nm with high positive charge. Thus, SFN-C 3 was applied for coating PEG400.

In order to form as SFN-CP, the SFN-C 3 was coated with PEG400. As shown in Figure 11B, SEM image of SFN-CP showed spherical particles with a smooth surface, which is similar to that of the SEM image of SFNs. While the DLS analysis showed a mean particle sizes ranging of SFN-CP from 185 nm to 198 nm with PI <0.2, depending on the amount of PEG400. Surface charge of SFN-CP showed positive zeta potential between +28.19 and +38.33 mV, as shown in Table 6. SFN-CP 4 was an optimum formulation and used for future experiment.

The entrapment efficacy (EE) of SFNs, the experiment was tightened up at the step of non-coating SFNs. We found that the EE of NaF was up to 95% at 7 μg/ml. While, the entrapment efficacy of NR was up to 67% at 1.2 μg/ml as shown in Table 7.

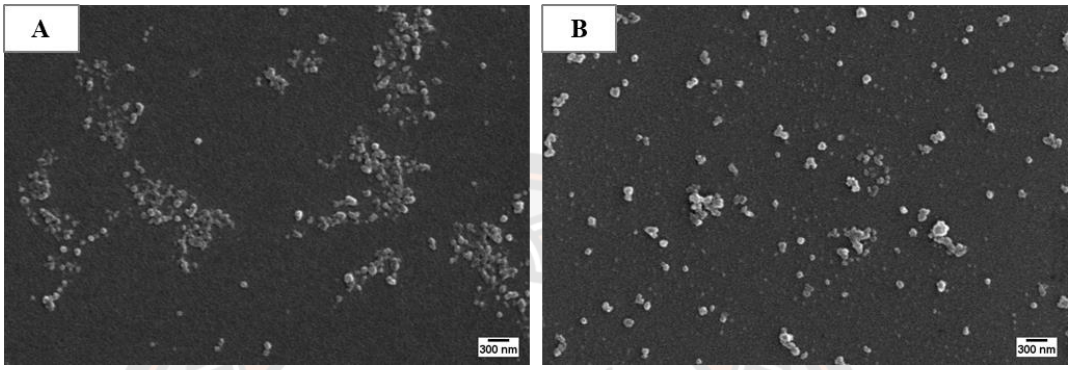

Figures 11 Micrographs showing scanning electron microscopy of (A) Silk fibroin nanoparticles (SFN 2) and (B) Silk fibroin nanoparticles coating CS and PEG400 (SFN-CP 4)

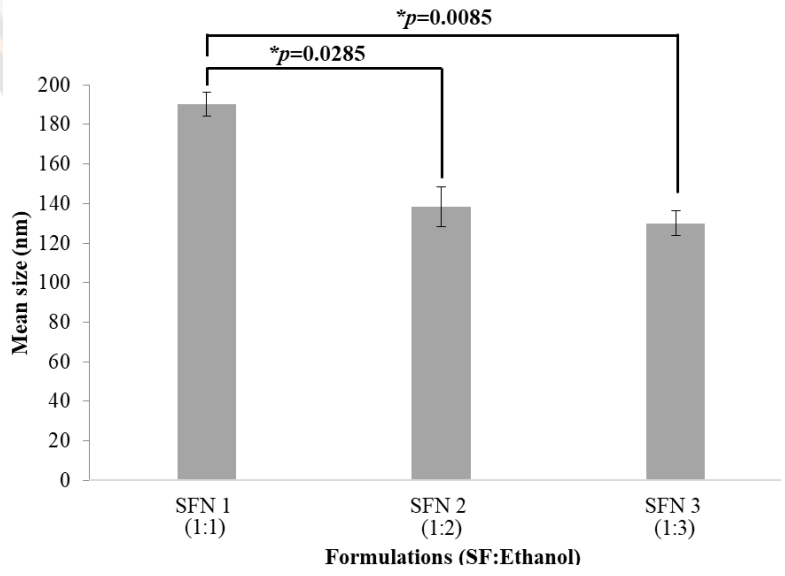

Figures 12 Effect of the volume ratios of SF: Ethanol on the mean particle size. SFN 1 significantly large size compared to SFN 2 and SFN 3 (Student's *t-test, p-value* <0.05). Error bars show the standard deviation (n=3).

Tables 4 Effect of the volume ratios of SF:Ethanol on the mean particle size, polydispersity index and zeta potential

Formulations	SF:Ethanol (ml)	Mean particle size (nm) ± SD	PI ± SD	Zeta potential (mV) ± SD	Turbidity
SFN 1	1:1	190.27 ± 6.01	0.172 ± 0.017	-20.21 ± 0.67	+ + + +
SFN 2	1:2	138.4 ± 10.16	0.147 ± 0.013	-20.93 ± 0.56	+ + +
SFN 3	1:3	130.03 ± 6.24	0.134 ± 0.038	-20.94 ± 1.02	+

Turbidity levels; very turbid (+ + + +), turbid (+ + +), fairly turbid (+).
PI; polydispersity index, SD; standard deviation, n = 3.

Tables 5 Effect of the volume ratios of SFN:CS for SFN-C on the mean particle size, polydispersity index and zeta potential (when the ratio of SF:Ethanol was fixed as 1:2).

Formulations	Amount of CS (mg/ml)	Mean particle size (nm) ± SD	PI ± SD	Zeta potential (mV) ± SD
SFN-C 1	0	138.40 ± 12.52	0.147±0.013	-20.93 ± 0.56
SFN-C 2	0.032	177.93 ± 12.52	0.177±0.022	+23.12 ± 5.68
SFN-C 3	0.625	193.87 ± 17.68	0.196±0.021	+34.02 ± 4.01
SFN-C 4	1.176	210.97 ± 35.96	0.216±0.029	+38.39 ± 4.88

PI; polydispersity index, SD; standard deviation, n = 3.

Tables 6 Effect of the amount of PEG400 on the mean particle size, polydispersity index and zeta potential (when the ratio SF: Ethanol was fixed as 1:2 and the amount of CS was fixed as 0.625 mg/ml)

Formulations	Amount of PEG400 (mg/ml)	Mean particle size (nm) ± SD	PI ± SD	Zeta potential (mV) ± SD
SFN-CP 1	0	193.87 ± 17.68	0.196 ± 0.021	+34.02 ± 4.01
SFN-CP 2	0.007	185.00 ± 26.76	0.168 ± 0.026	+28.19 ± 0.64
SFN-CP 3	0.017	183.07 ± 25.58	0.192 ± 0.033	+29.74 ± 1.31
SFN-CP 4	0.032	198.47 ± 35.54	0.162 ± 0.085	+38.33 ± 0.67

PI; polydispersity index, SD; standard deviation, n = 3.

Tables 7 Entrapment efficiency of drug models into the nanoparticles.

Formulations	Initial amount of model drug (µg/ml)	EE (%)	Concentration of drug in SFNs (mg/ml)
NaF-SFN 1	7	95.73	0.0067
NaF-SFN 2	10	69.81	0.007
NaF-SFN 3	30	59.20	0.018
NaF-SFN 4	60	45.71	0.027
NR-SFN 1	1.2	66.64	0.0008
NR-SFN 2	2.5	42.30	0.0011
NR-SFN 3	5	32.29	0.0016
NR-SFN 4	7	27.20	0.0019

EE; entrapment efficacy, NaF; sodium fluorescein, NR; nile red

The FTIR spectra of CS, SF, SFN 2 and SFN-CP 4 were shown in Figure 13. The conformation structure of the SFN 2 from random-coil and α-helix form (Silk I) into β-sheet crystalline (silk II) can be evaluated based on the wavenumber location of the absorption peak of amides. The peak shifted in amide I (C=O stretching) and II (N=H bending) band in FTIR spectra indicate a structural change from a random coil form to a β-sheet form (35-37). In this study, the absorption profile of SFN 2 demonstrated the spectral shifts in the amide I and amide II regions, 1624 and 1514 cm^{-1}, indicating a strong conformational change of SF from random coil to β-sheet structure. Hence, it is promising that the β-sheet structure of SF can be induced by ethanol. The SFN-CP 4 were prepared by used polyelectrolyte complexation technique with SFNs coated CS. The spectrum of CS showed N-H bending at 1631 cm^{-1} and 1598 cm^{-1} (2, 38). As expected, the spectrum of the SFN-CP 4 exhibited altered absorbance at the N-H groups, indicating a peak shifted on the amide I and amide II regions of SFN 2 and CS.

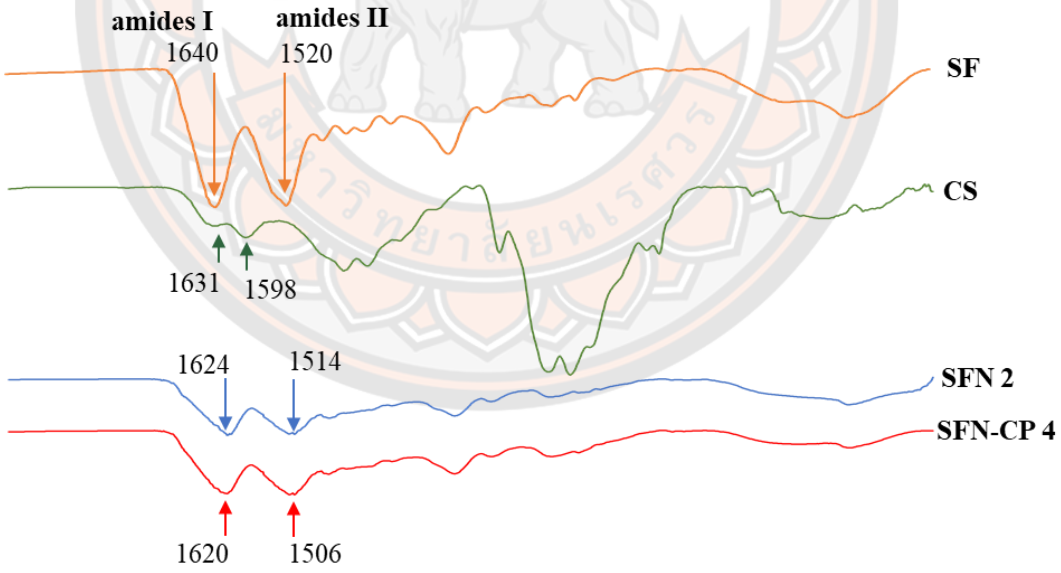

Figures 13 ATR-FTIR spectra of silk fibroin (SF), Chitosan (CS), Silk fibroin nanoparticles (SFN 2) and Silk fibroin nanoparticles coating CS and PEG400 (SFN-CP 4), focus on the amides I and II regions.

2. *Ex vivo* mucoadhesion study

The mucoadhesive properties of nanoparticles were investigated *ex vivo* using a porcine cornea. The FITC-SFN-CP showed good adhesion to the cornea of porcine as shown in Figure 14, while the solution form was cleared away at 60 min under continuous fluid flow. Interestingly, FITC-SFN-CP showed adherence to the corneal surface for up to 240 min compared to FITC solutions.

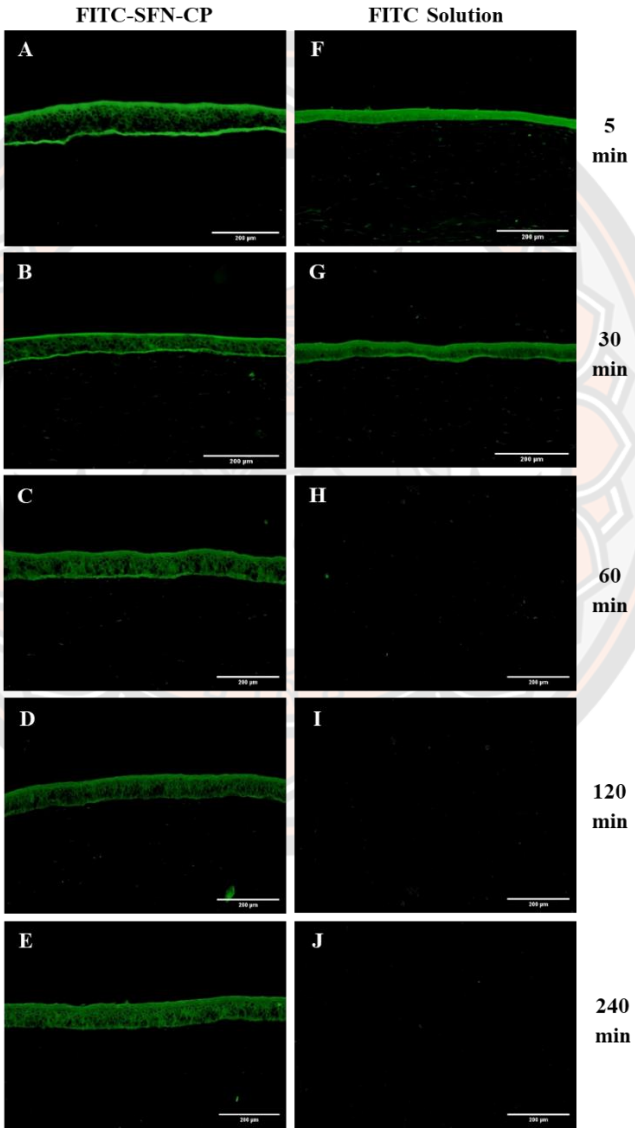

Figures 14 *Ex vivo* mucoadhesion study (A-E) showing fluorescence images of FITC- SFN-CP on the corneal surface. (F-J) Showing fluorescence images of FITC solution on the corneal surface. Scale bar = 200 µm.

3. Cell viability study

As shown in Figure 15, after treating with various concentration of SFN-CP 4 for 24 h, the HCEC cell showed viabilities of more than 90% in all concentration. While, the lowest concentration of SFN-CP 4, showed highest cell viability.

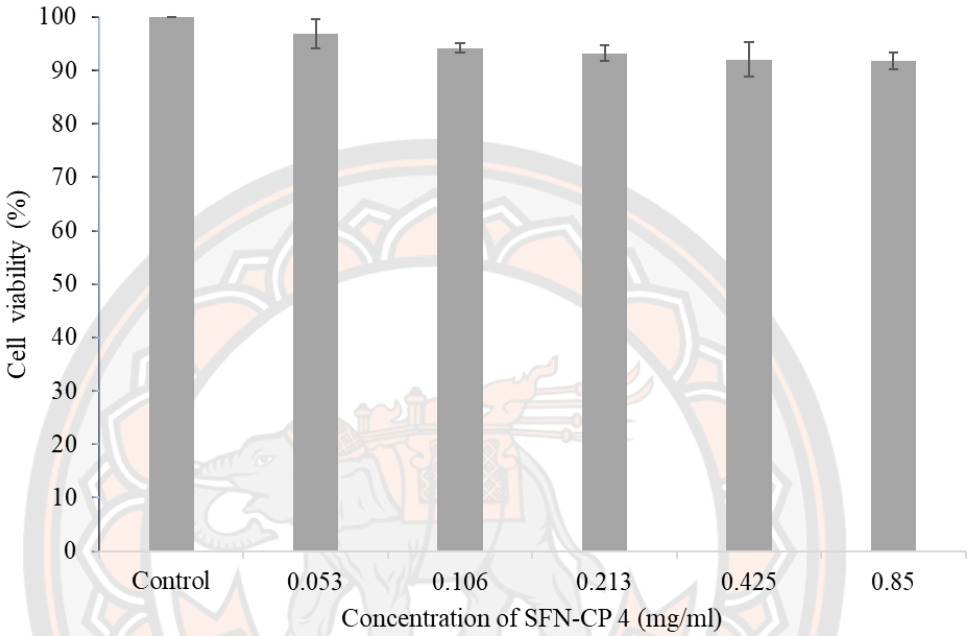

Figures 15 Effect of various concentrations of SFN-CP on the viability of HCEC (n=3). Cell viability (%) (y-axis) was measured after exposure to the various concentrations of SFN-CP (mg/ml) (x-axis)

4. Cellular uptake by HCEC cells

Since SFN-CP is not fluorescent, FITC-SFN-CP was used to monitor their possibility entering into HCEC, appearing in the green fluorescent signal. While, the nucleus of HCEC was stained with DAPI, appearing in the blue fluorescent signal. As show in figure 16, the intracellular green fluorescence of FITC-SFN-CP appears localized inside the cell within 5 min, and continued stay still visible in the cytoplasm until 240 min. These results indicate that FITC-SFN-CP are taken up and localized inside the HCEC.

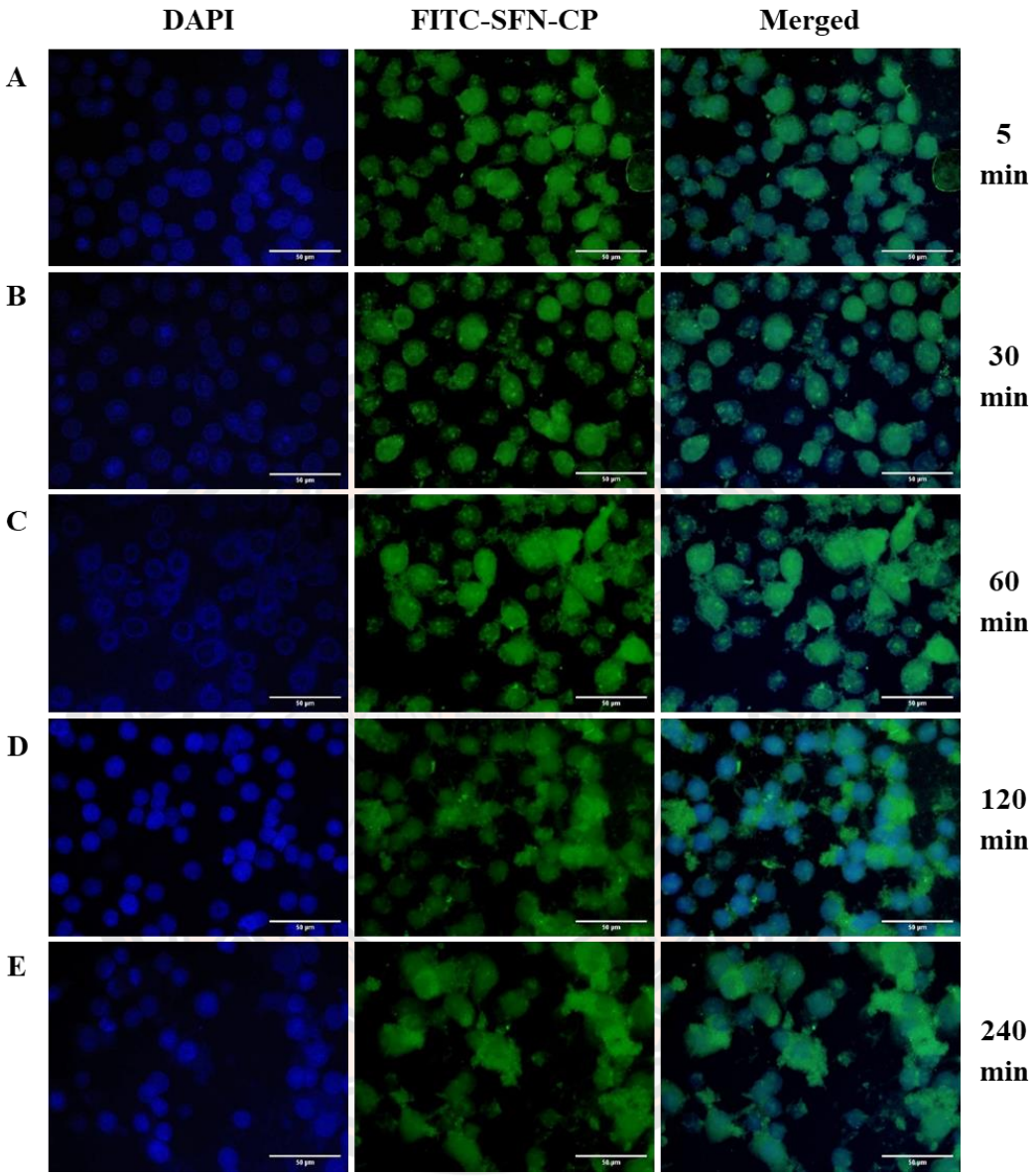

Figures 16 The HCEC image after exposure to FITC-SFN-CP for 5 min (A), 30 min (B), 60 min (C), 120 min (D), and 240 min (E). The nuclei of HCEC were stained with DAPI (Blue). Scale bar 50 μm, n=3.

CHAPTER V

DISCUSSIONS

The method for treatment of ocular surface disease is mostly administered topically as eye drops due to good patient compliance and non-invasive. However, the anatomical and physiological barriers of the eye are the major concerns with eye drops after topical administration, thereby resulting in low ocular bioavailability. Hence, to overcome these limitations and increase the ocular bioavailability, the formulations of eye drops should be designed to provide a prolonged drug residence time on the ocular surface, reduced drug elimination, and reduced toxicity to the ocular surface. In this study, the mucoadhesive SFN-CP were successfully developed for topical ocular drug delivery as a potential strategy to enhance the drug bioavailability on the ocular surface. SFN-CP showed able to enhance drug retention on ocular surface, reduced drug elimination, enter the cornea epithelial cells and non-toxic to the cells. The SFN-CP were easily prepared by combining the precipitation technique and the polyelectrolyte complexation technique. Silk fibroin was used as a negatively charged polymer and formed as nanoparticles by precipitation technique. While chitosan, a positively charged polymer, was used to coat the surface of nanoparticles by polyelectrolyte complexation technique. Addition, the obtained silk fibroin-chitosan nanocomplexes, were also covered with PEG400, a stabilizing agent, to enhance their stability in fluids. SEM image of SFN-CP was revealed spherical particles with smooth surface that may result in less or non-irritation to the ocular surface.

SFNs can be prepared using precipitation technique in ethanol and the effect of various volume ratios of SF:ethanol on their physiological properties were evaluated. In fact, the particles size and zeta potential (surface charge) are important for safe and effective on the ocular surface. Normally, the topical ocular drug should be particle size <10 μm due to larger particle size inducing irritation and eye discomfort (30, 36). In this study, all SFNs formulations showed a mean particle sizes <200 nm with PI <0.2, indicating the homogeneity of the prepared SFNs. The formulation SFN 1 showed significantly large size than SFN 2 and SFN 3. This is

probably due to a little volume of liquid silk solution was rapidly introduced into the ethanol, the nanometric silk globules formed at once. Hence, the small volume of ethanol could be induced the large aggregation of SF due to the surface tension increases, while the large volume of ethanol could be induced the smallest aggregates. Previously, likewise, it has been reported that the increasing of ethanol volume increasing ethanol concentration decreased the surface tension that caused a decrease in the particle size (39). Therefore, this study confirmed that the particle size decreases with increasing ethanol ratio. Moreover, all SFNs was not different on zeta potential, whereas a vast number of nanoparticles could be observed only in a formulation SFN 2 as a milky cloudy appearance. Thus, the SFN 2 was applied to the formulation prototype for coating with CS to form as SFN-C, using polyelectrolyte complexation technique, as well as loading drug models.

After determining the effect of various volume ratios of SFN:CS on the physiological properties of SFN-C. Our results demonstrate that the size of SFN-C was slightly increased with an increase volume of CS. The surface charge of all SFN-C shows positive surface charge more than 20 mV (Table 4). These results confirm that the positively charged CS was coated at the SFNs surface by interact with the negatively charged SF, resulting in charge switching from the negatively charged SFNs to positively charged SFN-C. As the formulation SFN-C 2 showed significantly small size than SFN-C 3 and SFN-C 4 (Table 5). However, the high zeta potential (greater than ±30 mV) of particles refers to their stability to resist the aggregation, flocculation, and coagulation (40). Thus, the formulation SFN-C 3 was selected for future experiments due to their smallest size with zeta potential greater than 30 mV.

PEG400 is commonly used as a stabilizing agent in the formulation of eye drops (1, 2). Hence, in case of nanoparticles stabilization preventing aggregation, a steric hindrance of polyethylene glycol 400 (PEG400) was considered and coated on the surface of SFN-C. No significant impact of PEG400 was seen on particle size, even increasing the volume ratios. In contrast, the particle surface charge was slightly increased when increasing PEG400. This is probably due to a change in pH increasing surface charge. As Table 6, the smallest size with positive zeta potential more than

30 mV could be observed at SFN-CP 4. Thus, SFN-CP 4 was indicated as an optimal formulation and used for FTIR, mucoadhesion test and cellular study.

The conformation structure of the SFNs from random-coil and α-helix form (silk I) into β-sheet crystalline (silk II) can be evaluated based on the wavenumber location of the absorption peak of amides. The peak shifted in amide I (C=O stretching) and II (N=H bending) band in FTIR spectra indicate a structural change from a random coil form to a β-sheet form (18, 20). In this study, the absorption profile of SFNs demonstrated the spectral shifts in the amide I and amide II regions, 1624 and 1514 cm^{-1}, indicating a strong conformational change of SF from random coil to β-sheet structure. SFN-CP 4 were formed by ionic interactions between the oppositely charged SFNs (-) and CS (+). FTIR spectra of SFN-CP 4 demonstrated the spectral shifts in the N-H and C=O absorption bands of CS and SFNs, respectively, confirmed the existence of the electrostatic interactions between the amine groups of CS and the carboxylic group of SFNs.

In order to investigate the potential of SFN-CP as carriers for drug delivery, NaF and NR were used as model drugs for a hydrophilic drug and a hydrophobic drug, respectively. Two model drugs were loaded only in the step of SFNs formation and the drug-unloaded was completely removed before CS coating. Hence, to tighten up our experiment, the entrapment efficiency was evaluated in the step of the optimum formulation of SFNs (SF:Ethanol as 1:2). As shown in Table 7, the significant difference in entrapment efficiency of among different concentrations of NaF and NR were not observed in this study. This is possibly due to the maximum capacity of the drugs that can be encapsulated is around 6.7 and 0.8 μg/ml for NaF and NR, respectively, depends on the properties of the fluorescein as the model drug. However, the best batch exhibited a high entrapment efficiency of up to 95.73% and 66.64% for NaF and NR, respectively.

Interestingly, SFN-CP could enhance the drug accumulation on the ocular surface due to its present mucoadhesive abilities. The FITC-SFN-CP showed good adhesion to the porcine corneal (*ex vivo*), while the solution form of FITC was cleared away after 30 min under continuous fluid flow. It is indicating that FITC could not adhere to the mucous membrane by itself. This is probably due to the negatively charged dye molecules of FITC would not interact with the negatively charged mucin.

However, in our study, FITC-SFN-CP exhibited a significant prolonged adherence more than 240 min at the surface of the porcine cornea. The mucoadhesive ability of FITC- SFN-CP might result from the net charge on the SFN-CP, which leads to electrostatic interactions between the positive charge by SFN-CP and negative charge by mucus of ocular surface. Moreover, PEG400 on SFN-CP formulations might be promote mucoadhesive through the hydrogen bond that binding with the mucin. Thus, it can be described that SFN-CP and the mucosal surface are closely bound by hydrogen bonding and physical entanglement (2).

Studies on cytotoxicity revealed that no cytotoxicity of SFN-CP could be observed in all concentrations (Figure 15). SFN-CP were made from SF and CS, there are biopolymer with non-toxic, biocompatible to cells. In addition, these materials were also used as a biopolymer for ophthalmic formulations with less cytotoxicity (1, 30). Moreover, the size of nanoparticles are very important for providing mechanistic details in the persistence and biological toxicity inside living cells. It has been reported that the size of nanoparticles smaller than 50 nm can easily enter most cells (with greater cytotoxicity) (41-43) and their larger surface area display tendency to agglomerate in the liquid, interact with molecules, such as proteins and DNA that may cause oxidation and DNA damage (43). In our study, the mean size of SFN-CP4 was 198 nm and exhibited non-toxic to HCEC. Similarly, it has been reported that the particles with sizes 100-200 nm did not show any toxicity even at relatively high concentrations (44). Thus, the SFN-CP exhibited a safe vehicle for topical ocular drug delivery.

Furthermore, SFN-CP were rapidly taken up by HCEC in the first 5 min and localized within the cytoplasm more than 4 hours (Figure 16). This indicates that SFN-CP could be internalized and may be further trafficked within the cell. Previously, it has been reported that silk fibroin nanoparticles can be uptaken by cells via endocytosis (45). Silk fibroin-derived particles enhance intracellular uptake and retention resulting in downmodulation of more than one pathway due to longer availability of the therapeutic (46, 47). While the presence of chitosan coating resulted in better cellular uptake and transcellular transport (1). Thus, more detailed investigations of SFN-CP are needed to further explore the uptake mechanisms and the trafficking within the cell.

CHAPTER VI

CONCLUSION

The mucoadhesive SFN-CP was successfully developed in this study. It exhibited spherical morphology, positive zeta potential with high entrapment of drug model up to 95%. At the optimal conditions, it showed a mean particle size of less than 200 nm, which is unlikely to cause any abrasive injury to the ocular surface. It exhibited a prolonged residence time at the ocular surface that can be improved the therapeutic efficacy of the topical solution drugs. Moreover, SFN-CP showed excellent *in vitro* biocompatibility without any detectable toxicity to HCEC after treatment and exhibited rapid cellular uptake. Overall, the mucoadhesive SFN-CP exhibit characteristics suitable for topical ocular drug delivery.

REFERENCES

REFERENCES

1. Chaiyasan W, Praputbut S, Kompella UB, Srinivas SP, Tiyaboonchai W. Penetration of mucoadhesive chitosan-dextran sulfate nanoparticles into the porcine cornea. Colloids and surfaces B, Biointerfaces. 2017;149:288-96.
2. Chaiyasan W, Srinivas SP, Tiyaboonchai W. Mucoadhesive chitosan-dextran sulfate nanoparticles for sustained drug delivery to the ocular surface. Journal of ocular pharmacology and therapeutics : the official journal of the Association for Ocular Pharmacology and Therapeutics. 2013;29(2):200-7.
3. Gaudana R, Ananthula HK, Parenky A, Mitra AK. Ocular drug delivery. The AAPS journal. 2010;12(3):348-60.
4. Silva MM, Calado R, Marto J, Bettencourt A, Almeida AJ, Goncalves LMD. Chitosan Nanoparticles as a Mucoadhesive Drug Delivery System for Ocular Administration. Marine drugs. 2017;15(12).
5. Jeevanandam J, Barhoum A, Chan YS, Dufresne A, Danquah MK. Review on nanoparticles and nanostructured materials: history, sources, toxicity and regulations. Beilstein J Nanotechnol. 2018;9:1050-74.
6. Lynch C, Kondiah PPD, Choonara YE, du Toit LC, Ally N, Pillay V. Advances in Biodegradable Nano-Sized Polymer-Based Ocular Drug Delivery. Polymers (Basel). 2019;11(8).
7. Narayan R. Nanobiomaterials: Nanostructured Materials for Biomedical Applications: Elsevier Science; 2017.
8. Du N, Liu XY, Narayanan J, Li L, Lim MLM, Li D. Design of superior spider silk: from nanostructure to mechanical properties. Biophys J. 2006;91(12):4528-35.
9. Dong Y, Dong P, Huang D, Mei L, Xia Y, Wang Z, et al. Fabrication and characterization of silk fibroin-coated liposomes for ocular drug delivery. European journal of pharmaceutics and biopharmaceutics : official journal of Arbeitsgemeinschaft fur Pharmazeutische Verfahrenstechnik eV. 2015;91:82-90.

10. Arkhipova AY, Kotlyarova MC, Novichkova SG, Agapova OI, Kulikov DA, Kulikov AV, et al. New Silk Fibroin-Based Bioresorbable Microcarriers. Bulletin of experimental biology and medicine. 2016;160(4):491-4.
11. Sogias IA, Williams AC, Khutoryanskiy VV. Why is Chitosan Mucoadhesive? Biomacromolecules. 2008;9(7):1837-42.
12. Brooks AE. The Potential of Silk and Silk-Like Proteins as Natural Mucoadhesive Biopolymers for Controlled Drug Delivery. Front Chem. 2015;3:65-.
13. Hanafy AF, Abdalla AM, Guda TK, Gabr KE, Royall PG, Alqurshi A. Ocular anti-inflammatory activity of prednisolone acetate loaded chitosan-deoxycholate self-assembled nanoparticles. International journal of nanomedicine. 2019;14:3679-89.
14. Srinivasarao DA, Lohiya G, Katti DS. Fundamentals, challenges, and nanomedicine-based solutions for ocular diseases. Wiley interdisciplinary reviews Nanomedicine and nanobiotechnology. 2018:e1548.
15. Drahanský M. Recognition of Eye Characteristics. Machine Learning and Biometrics2018.
16. Tsai CH, Wang PY, Lin IC, Huang H, Liu GS, Tseng CL. Ocular Drug Delivery: Role of Degradable Polymeric Nanocarriers for Ophthalmic Application. International journal of molecular sciences. 2018;19(9).
17. Lakhani P, Patil A, Majumdar S. Recent advances in topical nano drug-delivery systems for the anterior ocular segment. Therapeutic delivery. 2018;9(2):137-53.
18. Souto EB, Dias-Ferreira J, López-Machado A, Ettcheto M, Cano A, Camins Espuny A, et al. Advanced Formulation Approaches for Ocular Drug Delivery: State-Of-The-Art and Recent Patents. Pharmaceutics. 2019;11(9).
19. Tiwari R, Pandey V, Asati S, Soni V, Jain D. Therapeutic challenges in ocular delivery of lipid based emulsion. Egyptian Journal of Basic and Applied Sciences. 2018;5(2):121-9.
20. Cheng L, Muller SJ, Radke CJ. Wettability of silicone-hydrogel contact lenses in the presence of tear-film components. Current eye research. 2004;28(2):93-108.

21. Ali Y, Lehmussaari K. Industrial perspective in ocular drug delivery. Advanced drug delivery reviews. 2006;58(11):1258-68.
22. Weng Y, Liu J, Jin S, Guo W, Liang X, Hu Z. Nanotechnology-based strategies for treatment of ocular disease. Acta Pharm Sin B. 2017;7(3):281-91.
23. Shaikh R, Raj Singh TR, Garland MJ, Woolfson AD, Donnelly RF. Mucoadhesive drug delivery systems. J Pharm Bioallied Sci. 2011;3(1):89-100.
24. Shinkar DM, Dhake AS, Setty CM. Drug delivery from the oral cavity: a focus on mucoadhesive buccal drug delivery systems. PDA journal of pharmaceutical science and technology. 2012;66(5):466-500.
25. Khutoryanskiy VV. Advances in mucoadhesion and mucoadhesive polymers. Macromolecular bioscience. 2011;11(6):748-64.
26. Hombach J, Bernkop-Schnürch A. Mucoadhesive drug delivery systems. Handbook of experimental pharmacology. 2010(197):251-66.
27. Qi Y, Wang H, Wei K, Yang Y, Zheng R-Y, Kim IS, et al. A Review of Structure Construction of Silk Fibroin Biomaterials from Single Structures to Multi-Level Structures. International journal of molecular sciences. 2017;18(3):237.
28. Melke J, Midha S, Ghosh S, Ito K, Hofmann S. Silk fibroin as biomaterial for bone tissue engineering. Acta biomaterialia. 2016;31:1-16.
29. Xu Z, Shi L, Yang M, Zhu L. Preparation and biomedical applications of silk fibroin-nanoparticles composites with enhanced properties - A review. Materials Science and Engineering: C. 2019;95:302-11.
30. Chomchalao P, Nimtrakul P, Pham DT, Tiyaboonchai W. Development of amphotericin B-loaded fibroin nanoparticles: a novel approach for topical ocular application. Journal of Materials Science. 2020;55(12):5268-79.
31. Tran SH, Wilson CG, Seib FP. A Review of the Emerging Role of Silk for the Treatment of the Eye. Pharm Res. 2018;35(12):248-.
32. Mukhtar Ahmed KB, Khan MMA, Siddiqui H, Jahan A. Chitosan and its oligosaccharides, a promising option for sustainable crop production- a review. Carbohydrate Polymers. 2020;227:115331.

33. Bhatta RS, Chandasana H, Chhonker YS, Rathi C, Kumar D, Mitra K, et al. Mucoadhesive nanoparticles for prolonged ocular delivery of natamycin: In vitro and pharmacokinetics studies. International Journal of Pharmaceutics. 2012;432(1):105-12.
34. Dong Z, Cui H, Wang Y, Wang C, Li Y, Wang C. Biocompatible AIE material from natural resources: Chitosan and its multifunctional applications. Carbohydrate Polymers. 2020;227:115338.
35. Zhang Y-Q, Shen W-D, Xiang R-L, Zhuge L-J, Gao W-J, Wang W-B. Formation of silk fibroin nanoparticles in water-miscible organic solvent and their characterization. Journal of Nanoparticle Research. 2007;9(5):885-900.
36. Gonzalez-Mira E, Egea MA, Garcia ML, Souto EB. Design and ocular tolerance of flurbiprofen loaded ultrasound-engineered NLC. Colloids and Surfaces B: Biointerfaces. 2010;81(2):412-21.
37. Lozano-Pérez AA, Rivero HC, Pérez Hernández MdC, Pagán A, Montalbán MG, Víllora G, et al. Silk fibroin nanoparticles: Efficient vehicles for the natural antioxidant quercetin. International Journal of Pharmaceutics. 2017;518(1):11-9.
38. Chaiyasan W, Srinivas SP, Tiyaboonchai W. Crosslinked chitosan-dextran sulfate nanoparticle for improved topical ocular drug delivery. Mol Vis. 2015;21:1224-34.
39. Zhengbing Cao XC, Jinrong Yao, Lei Huang and Zhengzhong Shao. The preparation of regenerated silk fibroin microspheres. Soft Matter. 2007(7):910–5.
40. Joseph E, Singhvi G. Chapter 4 - Multifunctional nanocrystals for cancer therapy: a potential nanocarrier. In: Grumezescu AM, editor. Nanomaterials for Drug Delivery and Therapy: William Andrew Publishing; 2019. p. 91-116.
41. Das S, Mitra S, Khurana SMP, Debnath N. Nanomaterials for biomedical applications. Frontiers in Life Science. 2013;7(3-4):90-8.
42. Kong B, Seog JH, Graham LM, Lee SB. Experimental considerations on the cytotoxicity of nanoparticles. Nanomedicine (Lond). 2011;6(5):929-41.
43. Magdalena J EM. General Cytotoxicity and Its Application in Nanomaterial Analysis, Cytotoxicity. Tülay Aşkin Çelik, IntechOpen. 2017.

44. Yang P, Dong Y, Huang D, Zhu C, Liu H, Pan X, et al. Silk fibroin nanoparticles for enhanced bio-macromolecule delivery to the retina. Pharmaceutical development and technology. 2019;24(5):575-83.
45. Pham DT, Tiyaboonchai W. Fibroin nanoparticles: a promising drug delivery system. Drug Deliv. 2020;27(1):431-48.
46. Mathur AB, Gupta V. Silk fibroin-derived nanoparticles for biomedical applications. Nanomedicine (Lond). 2010;5(5):807-20.
47. Huang M, Ma Z, Khor E, Lim L-Y. Uptake of FITC-Chitosan Nanoparticles by A549 Cells. Pharmaceutical research. 2002;19(10):1488-94.

BIOGRAPHY